Oligomerization and Aggregation of Bovine Pancreatic Ribonuclease A: Characteristic Events Observed by FTIR Spectroscopy

Yong-Bin Yan,*† Jun Zhang,*† Hua-Wei He,*† and Hai-Meng Zhou*
*Department of Biological Sciences and Biotechnology, and †State Key Laboratory of Biomembrane and Membrane Biotechnology, Tsinghua University, Beijing 100084, China

ABSTRACT Nonnative protein aggregation, which is a common feature in biotechnology, is also a clinical feature in more than 20 serious degenerative diseases. We studied the specific events of bovine pancreatic ribonuclease A thermal aggregation by a combination of second derivative infrared analysis and two-dimensional infrared correlation spectroscopy. By comparing the events that occur in reversible and irreversible thermal unfolding processes, certain events that were related to protein aggregation were characterized. Particularly, a band that appeared at high temperatures was assigned to the cross β-structures in oligomers. The effect of pH, NaCl, and ethanol on ribonuclease A oligomerization as well as further aggregation induced by heat were studied and dissimilar effects of these additives were found. Basic pH and NaCl could accelerate the thermal aggregation but did not affect the formation of oligomers, whereas ethanol could increase both the aggregation rate and the population of oligomers. Our results suggested that the aggregation of RNase A might be initiated by hydrophobic interactions, controlled by oligomerization and mediated by electrostatic interactions. Moreover, the strategy of using second derivative and two-dimensional infrared analysis might provide a potential powerful tool to study the events that are directly related to the initiation of protein aggregation.

INTRODUCTION

Nonnative protein aggregation, which is a common feature in biotechnology (1,2), is also a clinical feature in more than 20 serious degenerative diseases (3–5) and has attracted considerable attention and effort in many research fields over the past several years (6,7). Though considerable progress has been made in recent years toward the understanding of the molecular mechanism of protein aggregation, particularly in amyloid fibrillation, the lack of data on the high-resolution structure of both regular and irregular aggregates limits the significance of those previously proposed mechanisms in intermolecular interactions between monomers (7–10). Moreover, the lack of detailed experimental data that could link the initial stage of aggregation and the final structure also limits the understanding of how aggregates form.

It has been widely accepted that the cross β-motif is the core structure that glues monomers together to form aggregates and the aggregation is a nucleation-controlled process. However, considerable debate exists as to how this cross β-motif is formed from the native protein structure. Questions such as ''do intermolecular interactions arise from the native structure, nonnative structure, or unfolded structure?'', ''how does the native α-helix convert to intermolecular β-sheet structures?'', ''what is the role of native β-sheet structures in aggregate formation?'', ''what determines whether a protein will aggregate or not when the environmental conditions are slightly changed?'', and 'why do some mutants aggregate easily, whereas others do not?'' are still quite difficult to answer. Moreover, in vivo research has indicated that cell toxicity might more likely be caused by prefibrillar aggregates than mature fibrils (11). Detailed information about the initial conformational changes during protein aggregation will lead to a better understanding of structural conversion related to protein aggregation and may facilitate the further development of strategies for preventing aggregation in vivo or in vitro.

Bovine pancreatic ribonuclease A (RNase A), a thoroughly studied model protein in folding, enzymology, structure (12), and oligomerization (10,13–17), has been shown to have the possibility to form amyloid fibrils by domain-swapping (10,15) and was chosen to investigate the mechanisms involved in the early stage of thermal aggregation. Because slightly different definitions have been correlated to protein oligomerization and aggregation in literature, it seems appropriate to point out that in this work, oligomerization means the formation of soluble nonnative oligomers, and aggregation means the formation of insoluble aggregates. The oligomerization studies in RNase A (10,15) as well as in degenerative disease-related proteins (18–20) have led to the hypothesis that domain-swapping is one of the important mechanisms of amyloid-like fibril formation. Moreover, previous studies have shown that the aggregation of RNase A is dependent on environmental conditions, such as pH, ion strength, or the existence of organic compounds (14,21–24). These properties suggest that the process of RNase A aggregation could be easily controlled and thus the events involved in the early stage of RNase A aggregation might be distinguished. Furthermore, the strategy of using one-dimensional (1D) and two-dimensional (2D) infrared (IR) analysis developed in this article might provide a

Submitted July 27, 2005, and accepted for publication October 24, 2005.

Address reprint requests to Dr. Yong-Bin Yan, Dept. of Biological Sciences and Biotechnology, Tsinghua University, Beijing 100084, People's Republic of China. Fax: 86-10-6277-1597; E-mail: ybyan@tsinghua.edu.cn.

0006-3495/06/04/2525/09 $2.00

doi: 10.1529/biophysj.105.071530

general method to study the events directly related to the initiation of protein aggregation.

MATERIALS AND METHODS

Sample preparation

Highly purified lyophilized bovine pancreatic ribonuclease A (type XII-A) was purchased from Sigma Chemical (St. Louis, MO) and used without further purification. Deuterated samples were from Cambridge Isotope Laboratories (Andover, MA). The infrared samples were prepared by dissolving the protein in D_2O at a concentration of 50 mg/ml in phosphate-buffered saline (PBS) buffer (containing 100 mM NaCl, 20 mM phosphate) or A-PBS buffer (containing 100 mM NaCl, 100 mM Na_2HPO_4 and 100 mM NaH_2PO_4). The pD values were read directly from an Orion pH meter (Orion Research, Beverly, MA) and no corrections were made for isotope effects. The fully deuterated RNase A samples were prepared by incubating the protein solutions in a water bath at 62°C for 15 min and the deuteration was checked by ^{1}H-NMR spectroscopy before use. All samples were lyophilized and were dissolved in D_2O before use with a final pD of 6.0 or 8.0 adjusted using DCl or NaOD. Samples containing 400 mM NaCl or 20% deuterated-ethanol were prepared by mixing the above samples and NaCl or ethanol stock solutions.

IR measurements

Details regarding the IR measurements were the same as those described before (25). In brief, all Fourier transform infrared (FTIR) spectroscopy experiments were measured on a PerkinElmer (Wellesley, MA) Spectrum 2000 spectrometer equipped with a dTGS detector; ~30 μl protein samples were placed between a pair of CaF_2 windows separated by a 50-μm Teflon spacer. Spectra were collected with a spectral resolution of 4 cm^{-1} in single-beam mode, and 256 or 128 scans were recorded. For thermal studies, spectra were recorded from 30°C to 90°C in increments of 2°C. For time-course studies, the samples were inserted into the spectrometer preequilibrated to the given temperatures, and spectra were recorded every 7.5 min after 7.5 min thermal equilibration.

1D and 2D IR analysis

Fourier self-deconvolution (FSD) was performed using the software Spectrum v3.02 provided by PerkinElmer with a gamma factor of 2.5 and a Bessel smoothing of 70%. Second derivative IR spectra were obtained using the algorithm in the software Spectrum v3.02 with a nine-point Savitzky-Golay smoothing. Kinetic data were obtained by using the quantitative second derivative infrared method developed by us recently (26). 2D IR synchronous and asynchronous correlation plots were computed using SDIAPP software developed in-house (25) according to the generalized 2D correlation algorithm (27). 2D IR correlation plots were constructed from nonnormalized FSD spectra with a spectral region of 1700–1600 cm^{-1}, and the time-averaged spectrum was used as a reference. The 2D correlation plots were presented as contour maps by drawing the contour lines every 10% off from the maximum intensity of the whole correlation map. The sequence of the events was characterized by analyzing the signs of the peaks in the 2D IR correlation plots using rules proposed by Noda (27–29). The band position was found to have a slight shift. However, this shift did not affect the 2D IR analysis since the shift was accompanied with the intensity change (30). The attempts to avoid artifacts in the 2D IR plots, which might be caused by baseline offsets, band overlapping, noise, or distortions in the spectra used for 2D correlation analysis, have been described in detail elsewhere (31). One more criterion was added, which stated that the results observed in 2D IR correlation plots should have corresponding events that could be distinguished in 1D IR analysis. These attempts were expected to prevent most of the pseudopeaks that might derive from noise or possible inappropriate 2D IR correlation plot construction.

RESULTS

Band assignment criteria

The secondary structure of RNase A has been studied by FTIR spectroscopy for many years (32–37). However, the assignment might also be confusing when there is a serious overlapping of bands from both native and unfolded structures in a thermal transition study. In this study, we developed two criteria for band assignment. First, the band assignment was referenced to the x-ray (38) or NMR structure (39) and the thermal behavior of a certain band. In general, the proportion of various secondary structures calculated from IR spectra should be consistent with that from x-ray or NMR structure. Moreover, a band should change continuously during a two-state structural transition. Secondly, the frequency pair of a certain secondary structure, such as the high- and low-frequency component of β-sheet structures, should reveal similar thermal properties. Thus if an apparent band is composed of two actual bands, they might be distinguished by their different thermal properties. These two criteria using the different stabilization properties of different secondary structures upon perturbation should also facilitate the band assignment in any conformational change studies. The correlation of FTIR bands and secondary structure of RNase A is presented in Table 1.

Characteristic events are responsible for the initiation of RNase A thermal aggregation

It has been shown that the thermal aggregation of RNase A is dependent on pH and could be promoted by the addition of salts (21–24). These properties suggested to us that it might be possible to distinguish the events directly related to aggregation by comparing the thermal transitions favoring reversible and irreversible unfolding. As presented in Figs. 1 and 2, the second derivative spectra of the samples in

TABLE 1 Correlation between the secondary structures and the amide I frequencies of RNase A at low and high temperatures

Band frequency (cm^{-1})	Assignment*	
	Below 60°C	Above 60°C
1611–1618	Side chains	Cross β-structures in aggregates
1625	Extended chains/β-sheet	Extended chains/β-sheet
1629–1639	β-Sheet	β-Sheet
1638	β-Sheet	Cross β-structures in oligomers
1644–1649	Random coil	Random coil
1650–1657	α-Helix	α-Helix
1660,1668,1674	β-Turns	β-Turns
1682	β-Sheet or turns	Cross β-structures in oligomers or aggregates

*Only the correlation between the IR bands and the dominant secondary structures in conformational changes were presented.

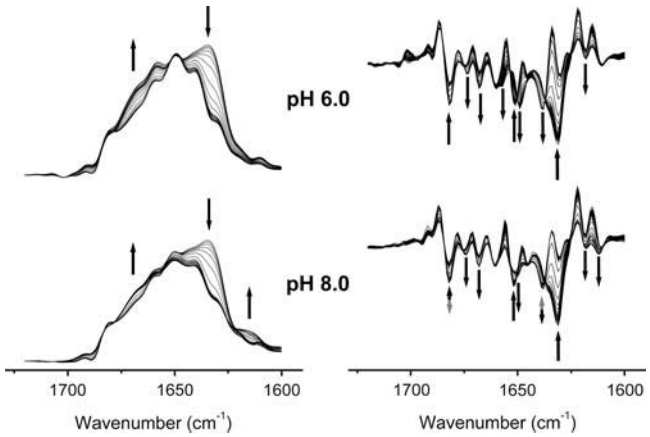

FIGURE 1 FSD (*left panel*) and second derivative (*right panel*) spectra of RNase A thermal denaturation in acidic (pD 6.0) and basic (pD 8.0) conditions. Fully deuterated samples were resolved in A-PBS. Only the FSD spectra above 60°C are shown in the left panel for clarity, whereas all second derivative spectra are shown in the right panel. The solid arrows indicate the direction of the intensity change of bands upon heating, and the shaded arrows indicate that the direction of intensity change was reversed at temperatures above 60°C. The arrows in the second derivative spectra are around bands at 1682, 1674, 1668, 1660, 1652, 1648, 1638, 1631, 1618, and 1612 cm^{-1}, from left to right, respectively.

A-PBS at a pD of 6.0 or 8.0 revealed similar properties in most bands including those at 1674 and 1668 cm^{-1} (nonnative β-turns), 1652 cm^{-1} (α-helix), 1631 cm^{-1} (β-sheet), and 1618 cm^{-1} (side chains). However, the changes of several bands including 1682, 1657, 1649, 1638, and 1612 cm^{-1} were quite different when subjected to heat stress (Table 2). The bands at 1682 and 1612 cm^{-1} had similar transitions at high temperatures and thus were assigned to the frequency pair of intermolecular β-sheet structures. The change of band around 1660 cm^{-1} above 70°C was similar to those at 1674 and 1668 cm^{-1}, and thus was assigned to nonnative β-turns formed at high temperatures. The band at 1638 cm^{-1} at temperatures above 70°C was assigned to intermolecular β-sheet structures in oligomers formed at high temperatures. The formation of these nonnative β-sheet structures could be attributed to the formation of nonnative β-sheet structures in monomers or the formation of oligomers through cross β-structures. There is no evidence that nonnative β-sheet structures in monomers could be formed by RNase A at high temperatures, whereas oligomerization was observed even in double-distilled water at high temperatures (14). Furthermore, the assignment of this band was confirmed by the observation of a small dimer peak in the fast protein liquid chromatography spectra (data not shown) similar to those in literature (14) and by the slight intensity increase of the β-sheet structures in the oligomer-enriched state induced by lyophilization from 40% acetic acid (40). Thus the explanation that the intensity increase at 1638 cm^{-1} was due to oligomerization of RNase A at high temperatures is likely to be true. This assignment was also consistent with the well-known mechanism, which indicates that the formation of the nucleus is the key step in protein aggregation (6). Based on the above assignment, the events that are directly related to aggregation could be described as the formation of the 1612 cm^{-1} band from aggregates along with the change of the 1638 cm^{-1} band from cross β-structures in oligomers. The conditions that favored aggregation (in this case, pD 8.0) resulted in fewer nonnative β-turns and random coils than in the conditions that favored reversible unfolding (in this case, pD 6.0).

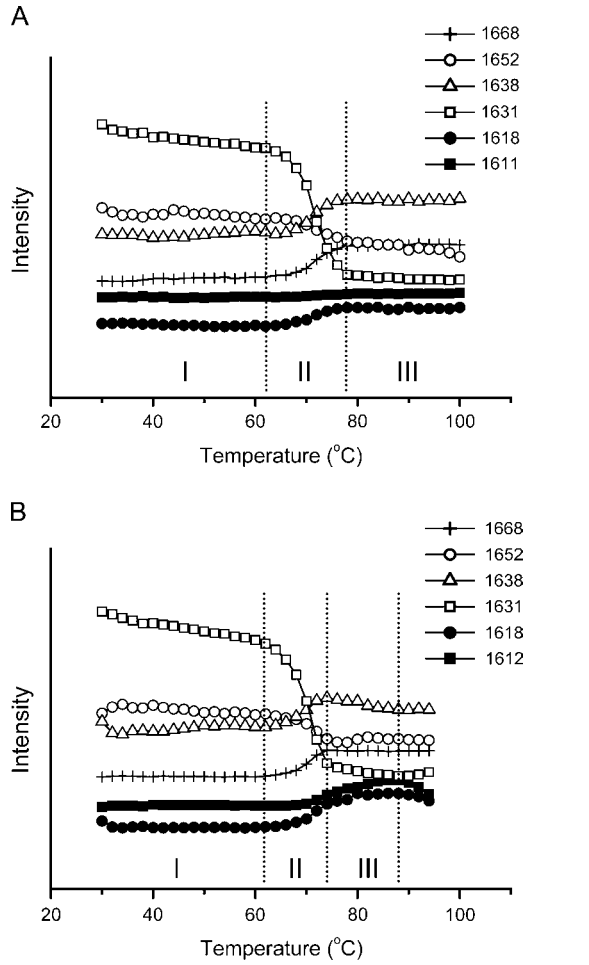

FIGURE 2 Comparison of the conformational changes of RNase A thermal denaturation in acidic (*A*) and basic (*B*) conditions. The intensity of certain bands was obtained from the second derivative spectra using the quantitative second derivative infrared method (26). Periods I–III correspond to the ''pretransitional stage'', ''major unfolding stage'', and ''residual unfolding stage'' or ''early aggregation stage'', respectively. All other conditions were the same as those in Fig. 1.

Sequential events from 2D IR correlation analysis

The above analysis based on the intensity change of bands in second derivative spectra suggested that the distinct events could be related to the early stage of RNase A thermal aggregation. However, this analysis could not be used to correlate the aggregation events and the conformational changes. Thus 2D IR correlation analysis, which has been shown to be

TABLE 2 A comparison of the intensity changes of the dominant amide I bands of RNase A during thermal denaturation at various conditions

Band frequency (cm^{-1})	Period II*			Period III		
	pD 6.0	pD 8.0	pD 8.0 (NaCl)	pD 6.0	pD 8.0	pD 8.0 (NaCl)
1612	—†	↑	↑	—	↑	↑
1618	↑	↑	↑	—	↑	—
1631	↓	↓	↓	—	↘	↘
1638	↑	↑	↑	—	↘	↓
1648	↑	↗	—	—	—	—
1652	↓	↓	↓	↘	—	↓
1668, 1674	↑	↑	↑	—	—	—
1682	↓	↓	↓	—	↑	↑

*Period II and Period III are the same as those defined in Fig. 2 and Fig. 4.
†The symbol ''—'' represents no significant change, ''↑'' represents intensity increase, ''↓'' represents intensity decrease, ''↗'' represents a slight increase of the band intensity, and ''↘'' represents a slight decrease of the intensity of the corresponding band that was observed.

a powerful tool in protein thermal transition studies (41), was used to further characterize the order of the events. In general, the synchronous spectrum contains auto peaks that located on the diagonal and crosspeaks that are off-diagonally placed, whereas asynchronous 2D correlation is characterized by asymmetric crosspeaks. The auto peaks in the synchronous spectrum indicated that the corresponding band has an intensity change upon perturbation. The crosspeaks in the synchronous plot reflect that the correlated bands change simultaneously upon perturbation and the sign (positive or negative) indicate the correlated events vary in the same or opposite direction. In the asynchronous plot, the crosspeaks are formed only between those bands whose intensity evolves independently, and a positive cross peak at (v_1, v_2), where $v_1 < v_2$, suggests that the change of the band at v_1 precedes the change of the band at v_2 and vice versa for a negative crosspeak (27–29).

Periods I, II, and III defined in Fig. 2 represent the so-called ''pretransitional stage'', ''major unfolding stage'', and ''residual unfolding stage'' or ''early aggregation stage'', respectively. Consistent with the results from 1D FTIR analysis, no significant difference was found in the pretransitional stage between the two samples, and the 2D IR correlation plots of Period I are not shown here. During the major unfolding stage (Period II), as presented in Fig. 3, *A* and *C*, the synchronous plots were almost identical, whereas quite different band patterns were developed in the asynchronous plots. Based on the band assignment results above, the appearance of the crosspeak at 1633/1667 cm^{-1} in Fig. 3, *A*-Φ and *C*-Φ, suggested that the formation of nonnative β-turns and unfolding of native β-sheet structures were the dominant events in this stage for proteins either at acidic pH or at basic pH. The main asynchronous events for the protein in acidic conditions (Fig. 3 *A*-Ψ) were correlated to the change of the band at 1633 cm^{-1}, and intense peaks were found at 1625/1633 and 1633/1640 cm^{-1}. Weak peaks could also be found at 1633/1653, 1628/1665, and 1612/1633 cm^{-1}. The signs of these peaks indicated that the order of events during this stage was 1653 cm^{-1} (native α-helices) > 1633 cm^{-1} (native β-sheet structures) > 1612 (side chains), 1625 (extended chains), and 1640 cm^{-1} (cross β-structures in oligomers) > 1665 cm^{-1} (nonnative turns). Strikingly different from Fig. 3 *A*-Ψ, only two main crosspeaks, 1616/1633 and 1633/1651, could be found in the asynchronous plot for the sample under basic pH conditions (Fig. 3 *C*-Ψ).

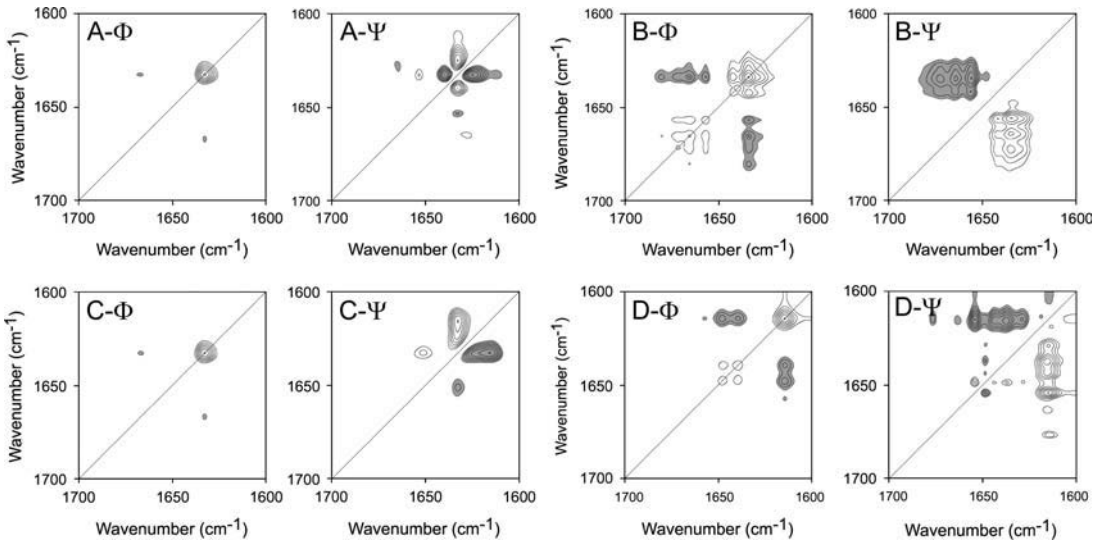

FIGURE 3 2D correlation analysis of the IR spectra of RNase A thermal denaturation in acidic (*A* and *B*) and basic (*C* and *D*) conditions. Synchronous (Φ) and asynchronous (Ψ) plots were constructed from the corresponding spectra recorded in Period II (*A* and *C*) and III (*B* and *D*) defined in Fig. 2. Period II corresponds to the temperature range of 62–76°C (*A*, pD 6.0) or of 62–74°C (*C*, pD 8.0), whereas Period III corresponds to the temperature range of 78–100°C (*B*, pD 6.0) or 76–84°C (*D*, pD 8.0). Clear and dark peaks represent positive and negative, respectively.

The signs of these peaks indicated that the order of events for the sample under basic pH conditions (Fig. 3 *C*-Ψ) was 1651 cm^{-1} (native α-helices) > 1633 cm^{-1} (native β-sheet structures) > 1617 (intermolecular β-sheet structures). The results from 2D IR correlation analysis at this stage were quite consistent with those from 1D IR spectra except that the order of the events could be obtained by 2D IR.

During the residual unfolding stage (Period III), the development of different patterns of both synchronous and asynchronous events was found in 2D IR correlation plots for the two samples. For the sample at pD 6.0, the main events occurring in this stage (Fig. 3 *B*-Φ) were the unfolding of the native β-sheet structures (1634 cm^{-1}) and the formation of nonnative β-turns (1657, 1665, and 1681 cm^{-1}). The signs in Fig. 3 *D*-Ψ suggested that the unfolding of the native structures preceded the formation of nonnative structures. For the sample at pD 8.0, the 2D IR correlation plots were more complicated due to the formation of both disordered structures and aggregates. A close inspection of signs in the asynchronous plot (Fig. 3 *D*-Ψ) indicates that the aggregation bands (1617 and 1682 cm^{-1}) and the disordered bands (1649 cm^{-1}) were formed along with the change of bands at 1629, 1637, 1644, and 1654 cm^{-1}. The appearance of crosspeaks at 1614/1639 and 1614/1648 cm^{-1} in the synchronous plot (Fig. 3 *D*-Φ) indicated that the change of cross β-structures in aggregates and that of cross β-structures in oligomers and disordered structures occurred simultaneously but in opposite directions. The sequence of events suggested that the structures that changed before the initiation of aggregation were likely to be the residual structures of the protein at high temperatures including residual helices (1654 cm^{-1}), β-sheet structures (1629 and 1637 cm^{-1}), and turns (1677 cm^{-1}). Consistent with the result from 1D IR spectra, the most significant event at this stage for the sample at basic conditions was the opposite intensity change of the band from cross β-structures in aggregates and in oligomers.

It is noteworthy that previous studies have suggested that the irreversible thermal inactivation of RNase A at neutral pH was mainly due to the disulfide interchange (22). However, this is not the case for the initiation of RNase A aggregation since the appearance of aggregation was found to occur at ~20°C lower than the temperature used by Zale and Klibanov. Of course, it is possible that the disulfide interchange plays a crucial role in the formation of large aggregates of RNase A at high temperatures above 90°C, as suggested by Meersman and Heremans (42). In this research, the aggregation was found to be closely associated with the oligomerization of the protein at high temperatures by both 1D and 2D IR analysis.

NaCl could increase the aggregation rate but not the population of the oligomers

It has been shown that many salts, such as NaCl, could promote the aggregation of many proteins (2), including RNase A (23,24). A sample in which RNase A was dissolved in A-PBS (pD 8.0) with the addition of 400 mM NaCl was prepared and studied by the methods used above. No difference was found in the events involved in aggregation with or without the addition of NaCl (Fig. 4; see also Table 2). However, the amount of aggregates was somewhat increased when compared with the intensity of the band around 1612 cm^{-1}, whereas the intensity of the band around 1638 cm^{-1} gradually decreased at temperatures above 72°C (see also Table 2). The maximum of the intensity of the band at 1638 cm^{-1} moved from 74°C to 72°C with the addition of 400 mM NaCl. This slight difference should be attributed to the fast decrease of this band because no such phenomena were observed for the native bands or aggregation bands. These results suggested that the addition of NaCl had no significant effect on either the sequence of events or the thermal stability of the protein, whereas the promotion effect of NaCl on aggregation could be due to the increasing of the aggregation rate. It is noteworthy that a fourth period (Period IV) was defined in Fig. 4 and this period was identified by the observation that no intensity decrease was found at 1638 cm^{-1}, whereas an intensity increase could still be observed at 1612 cm^{-1}. Thus, this period was tentatively called the ''further aggregation stage''.

It is well known that the formation of soluble oligomers formed by either specific or nonspecific interactions between molecules in the lag phase might be important to protein aggregation (2,6). It is interesting that the formation of oligomers was observed in all samples even if the sample had no tendency to aggregate. This phenomenon was also consistent with the previous study by Gotte et al. (14), which indicated that pH has little effect on RNase A oligomerization, and the C-terminal dimer can be observed even in very acidic conditions. The RNase A oligomers were very stable at high temperatures in conditions where aggregation was not favored (see Fig. 2). The effect of pH and salts on the

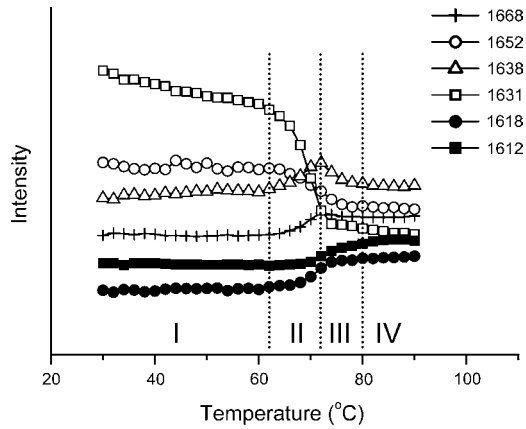

FIGURE 4 Effect of NaCl on the thermal transitions of RNase A. The protein was dissolved in A-PBS with the addition of 400 mM NaCl. Details regarding the experiment and data processing were the same as those in Fig. 2.

thermal behavior of RNase A had been attributed to their effect on electrostatic interactions of the molecules (2,23,24). These results further suggested that this effect did not affect the formation of RNase A oligomers but mainly affected the amounts of oligomers sticking together.

Ethanol could increase both the aggregation rate and the population of the oligomers

Unlike salts, ethanol or many other organic compounds have the ability to change the conformation states as well as the thermal stability of proteins (2). It has been shown that RNase A could form quite large amounts of oligomers in buffered ethanol solutions when incubated at high temperatures (14). Particularly, the addition of ethanol could significantly increase the number of dimers or trimers swapped in the C-terminal domain. In this research, time-course studies at 70°C were carried out for samples prepared by dissolving the protein in A-PBS with the addition of ethanol. No aggregation (as indicated by the band around 1612 cm^{-1}) was found for the sample in absence of ethanol after heated at 70°C for 2 h. The addition of ethanol accelerated the thermal aggregation of RNase A in a concentration dependent manner (see Supplemental Fig. 2). As shown by the thermal transition experiments (see Fig. 4) and those by Gotte et al. (14), the addition of NaCl did not affect the formation of oligomers, but is more like to prompt the oligomers to stick together. Thus the time course experiment of the protein in the presence of 400 mM NaCl was taken as a control to characterize the effect of ethanol. A comparison of the effect of NaCl and ethanol on RNase A thermal aggregation was shown in Fig. 5. Three stages in the time-course aggregation of RNase A could be clearly distinguished. Stage *i* was the initial aggregation stage that was defined as aggregation followed by the fast denaturation of the native structure and accompanied by the formation of the oligomers (indicated by a band at 1638 cm^{-1}), whereas stage *ii* was defined as aggregation followed by the decrease of the oligomers and further unfolding of the native structure. The aggregation was very fast in these two stages, whereas it slowed down in stage *iii*, which was defined as further aggregation without significant changes in the other structures. These three stages characterized here are quite consistent with the model of $N \leftrightarrow U \rightarrow O \rightarrow A$, where N, U, O, and A represent the native, unfolded, nonnative oligomers and large aggregate states. For the protein in buffer with 20% ethanol, stage *i* was very short, and meanwhile the aggregation bands were more intense than that with 400 mM NaCl, which suggested that the protein was gradually destabilized by ethanol (14). A relatively higher number of oligomers (indicated by the band at 1638 cm^{-1}) was found in Fig. 5 *C* than that in Fig. 5 *B*, which suggested that the fast aggregation of RNase A in the presence of ethanol could be attributed to both the destabilization effect of the native structures and the promotion effect on the formation of oligomers. Moreover, the phenomenon that the intensity increase of the band from aggregates is accompanied with the intensity decrease of the band from oligomers (Fig. 2 and 3) also suggested that the oligomers might be the precursors of the aggregates. This conclusion is quite consisted with those previous studies (2–4, 6).

Microenvironments of Tyr and Asp residues

The IR spectra of proteins also have several characteristic ''markers'' of amino acid side chains, including the band around 1515 cm^{-1}, the marker of the Try side chain, and the band around 1584 cm^{-1}, the marker of the Asp side chain (43). It is also possible to identify whether these amino acids were involved in RNase A aggregation by monitoring the band shift of these ''markers''. As presented in Fig. 6 *B*, the peak shift of the Asp band of the two samples has similar two-state transitions upon heating. These two melting curves also coincide with the unfolding transition of secondary structures revealed in Fig. 2, which suggested that the Asp side chains were not involved in the initiation of RNase A aggregation. The Tyr marker band at 1515 cm^{-1} of the sample at pD 6.0 also shows a typical two-state transition. This result was quite consistent with those in literature (35,44,45). However, the Tyr band of the sample at pD 8.0 could not be interpreted by a simple two-state model. The sharp red-shift above 72°C suggested that at least one Tyr side chain was in a more buried environment upon aggregation (see also Fig. 2 *B*). The 2D IR correlation analysis of the Period III in Fig. 2 *B* also indicated that the formation of aggregates occurred before the environmental change of Tyr residues by the existence of an asynchronous peak located at

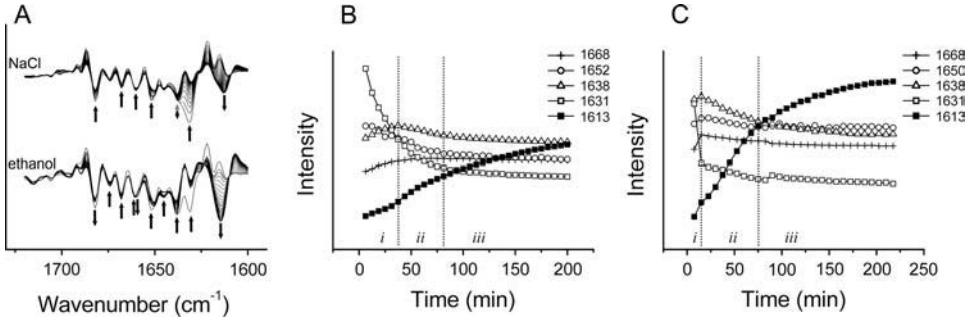

FIGURE 5 Effect of NaCl or ethanol on the time-course thermal aggregation of RNase A at 70°C. The second derivative spectra (*A*) and the intensity change of certain bands with the addition of 400 mM NaCl (*B*) or 20% ethanol (*C*) are presented. Details regarding the experiment and data processing were the same as those in Fig. 1 and 2.

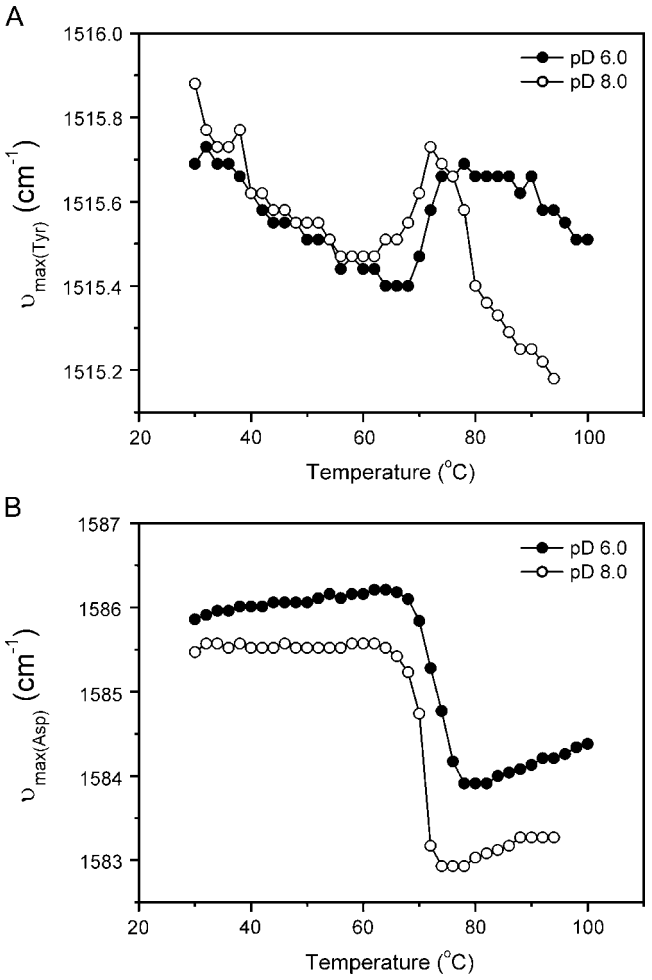

FIGURE 6 Peak shift of the marker bands of Tyr (*A*) and Asp (*B*) side chains during RNase A thermal denaturation. The protein was tested in acidic conditions (●) or basic conditions (○) as a function of temperature. The maximum wavenumbers around 1515 and 1584 cm^{-1} were directly measured in the original spectra.

1614/1515 cm^{-1} (see Supplemental Fig. 3). It is impossible to determine which Tyr was involved in the initiation of RNase A aggregation from our research. However, a combination of the results in this study and previous observations might provide some clues. To stick together, the hydrophobic region that initiates aggregation must unfold or be exposed to solvent first (46–49). Previous reversible thermal unfolding studies have indicated that the thermal transition of RNase A involves multiple steps (50,51) and the C-terminal region unfolds at higher temperatures than the change of Tyr side chains (52). There are six Tyr residues in RNase A, and two of these, Tyr-97 and Tyr-115, are located near the interface of thermally induced dimers (10,53). Thus it is more likely that Tyr-97 or/and Tyr-115 might be involved in the initiation of aggregation. This conclusion also coincides with the hypothesis proposed by Liu et al. (10) that the hinge loop region (residues 112–115) is responsible for the possible Amyloid-like fibril formation of RNase A. Moreover, the

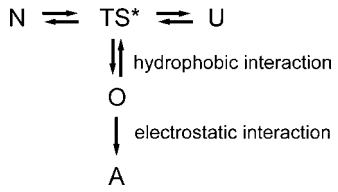

SCHEME 1 Possible mechanism of RNase A thermal aggregation. *N* is the native state, *TS** is the transition state, *U* is the unfolded state, *O* represents the oligomers, and *A* is the aggregates.

properties of the oligomers characterized in this article and those in previous oligomerization studies (14) were quite similar except that the domain-swapped oligomers were characterized under room temperature where the protein might be able to refold to native-like structures. Thus it might be safe to conclude that cross β-structures in oligomers are formed by the C-terminal segment of RNase A, although this conclusion is tentative and needs further investigations.

CONCLUSIONS

It has been proposed by Liu et al. (10,15) that RNase A might form amyloid fibrils through the swapping of C-terminal β-strands based on the observation of crystal structures of oligomers. The results herein support the assumption that the oligomers formed by the C-terminal segment were the precursors of aggregates. Moreover, detailed information concerning the early stage of thermal aggregation was obtained by a careful selection of the system that could be easily controlled and could be correlated to those events that are responsible for aggregation. The results here suggested that the aggregation of RNase A was initiated by hydrophobic interactions, controlled by oligomerization, and mediated by electrostatic interactions. This mechanism is summarized in Scheme 1, where *N* is the native state, *TS** is the transition state, *U* is the unfolded state, *O* represents the oligomers, and *A* is the aggregates. In such a mechanism, it is imaginable that the aggregation will be accelerated by salts such as NaCl, which mainly affect the electrostatic interactions, and by organic compounds like ethanol that stabilize the oligomers. It is noteworthy that this study also indicated the probability of the existence of structural rearrangement before aggregation, which suggested that some of the features of the early stage might not be obtained from the structural studies of mature aggregates. The results herein provide an improved understanding of how aggregation is initiated and may facilitate the further development of strategies to prevent aggregation both in vivo and in vitro.

SUPPLEMENTARY MATERIAL

An online supplement to this article can be found by visiting BJ Online at http://www.biophysj.org.

The authors thank Prof. Su-Qin Sun (Tsinghua University, People's Republic of China) for her help with the IR measurements, and Prof. Massimo Libonati (Università di Verona, Italy) for stimulating discussions.

This investigation was supported by funds from the National Natural Science Foundation of China (No. 30500084) and the National Key Basic Research Special Foundation of China (No. G1999075607).

REFERENCES

1. Dong, A., S. J. Prestrelski, S. D. Allison, and J. F. Carpenter. 1995. Infrared spectroscopic studies of lyophilization- and temperature-induced protein aggregation. *J. Pharm. Sci.* 84:415–424.
2. Chi, E. Y., S. Krishnan, T. W. Randolph, and J. F. Carpenter. 2003. Physical stability of proteins in aqueous solutions: mechanism and driving forces in nonnative protein aggregation. *Pharm. Res.* 20:1325–1336.
3. Horwich, A. 2002. Protein aggregation in disease: a role for folding intermediates forming specific multimeric interactions. *J. Clin. Invest.* 110:1221–1232.
4. Merlini, G., and V. Bellotti. 2003. Molecular mechanisms of amyloidosis. *N. Engl. J. Med.* 349:583–596.
5. Stefani, M., and C. M. Dobson. 2003. Protein aggregation and aggregate toxicity: new insights into protein folding, misfolding diseases and biological evolution. *J. Mol. Med.* 81:678–699.
6. Dobson, C. M. 2003. Protein folding and misfolding. *Nature.* 426:884–890.
7. Tycko, R. 2004. Progress towards a molecular-level structural understanding of amyloid fibrils. *Curr. Opin. Struct. Biol.* 14:96–103.
8. Perutz, M. F., T. Johnson, M. Suzuki, and J. T. Finch. 1994. Glutamine repeats as polar zippers: their possible role in inherited neurodegenerative disease. *Proc. Natl. Acad. Sci. USA.* 91:5355–5358.
9. Lazo, N. D., and D. T. Downing. 1998. Amyloid fibrils may be assembled from β-helical protofibrils. *Biochemistry.* 37:1731–1735.
10. Liu, Y., G. Gotte, M. Libonati, and D. Eisenberg. 2001. A domain-swapped RNase A dimer with implications for amyloid formation. *Nat. Struct. Biol.* 8:211–214.
11. Walsh, D. M., I. Klyubin, J. V. Fadeeva, W. K. Cullen, R. Anwy, M. S. Wolfe, M. J. Rowan, and D. J. Selkoe. 2002. Naturally secreted oligomers of amyloid β protein potently inhibit hippocampal long-term potentiation in vivo. *Nature.* 416:535–539.
12. Raines, R. T. 1998. Ribonuclease A. *Chem. Rev.* 98:1045–1065.
13. Gotte, G., M. Bertoldi, and M. Libonati. 1999. Structural versatility of bovine ribonuclease A: distinct conformers of trimeric and tetrameric aggregates of the enzyme. *Eur. J. Biochem.* 265:680–687.
14. Gotte, G., F. Vottariello, and M. Libonati. 2003. Thermal aggregation of ribonuclease A. A contribution to the understanding of the role of 3D domain swapping in protein aggregation. *J. Biol. Chem.* 278:10763–10769.
15. Liu, Y., G. Gotte, M. Libonati, and D. Eisenberg. 2002. Structures of the two 3D domain-swapped RNase A trimers. *Protein Sci.* 11:371–380.
16. Nenci, A., G. Gotte, M. Bertoldi, and M. Libonati. 2001. Structural properties of trimers and tetramers of ribonuclease A. *Protein Sci.* 10:2017–2027.
17. Libonati, M., and G. Gotte. 2004. Oligomerization of bovine ribonuclease A: structural and functional features of its multimers. *Biochem. J.* 380:311–327.
18. Knaus, K. J., M. Morillas, W. Swietnicki, M. Malone, W. K. Surewicz, and V. C. Yee. 2001. Crystal structure of the human prion protein reveals a mechanism for oligomerization. *Nat. Struct. Biol.* 8:770–774.
19. Janowski, R., M. Kozak, E. Jankowska, Z. Grzonka, A. Grubb, M. Abrahamson, and M. Jaskolski. 2001. Human cystatin C, an amyloidogenic protein, dimerizes through three-dimensional domain swapping. *Nat. Struct. Biol.* 8:316–320.
20. Staniforth, R. A., S. Giannini, L. D. Higgins, M. J. Conroy, A. M. Hounslow, R. Jerala, C. J. Craven, and J. P. Waltho. 2001. Three-dimensional domain swapping in the folded and molten-globule states of cystatins, an amyloid-forming structural superfamily. *EMBO J.* 20:4774–4781.
21. Hermans, J., and H. A. Scheraga. 1961. Structural studies of ribonuclease. V. Reversible change of configuration. *J. Am. Chem. Soc.* 83:3283–3292.
22. Zale, S. E., and A. M. Klibanov. 1986. Why does ribonuclease irreversibly inactivate at high temperatures? *Biochemistry.* 25:5432–5444.
23. Tsai, A. M., J. H. van Zanten, and M. J. Betenbaugh. 1998. I. Study of protein aggregation due to heat denaturation: a structural approach using circular dichroism spectroscopy, nuclear magnetic resonance, and static light scattering. *Biotechnol. Bioeng.* 59:273–280.
24. Tsai, A. M., J. H. van Zanten, and M. J. Betenbaugh. 1998. II. Electrostatic effect in the aggregation of heat-denatured RNase A and implications for protein additive design. *Biotechnol. Bioeng.* 59:281–285.
25. Yan, Y.-B., Q. Wang, H.-W. He, X.-Y. Hu, R.-Q. Zhang, and H.-M. Zhou. 2003. Two-dimensional infrared correlation spectroscopy study of the heat induced unfolding and aggregation process of myoglobin. *Biophys. J.* 85:1959–1967.
26. Zhang, J., and Y.-B. Yan. 2005. Probing conformational changes of proteins by quantitative second derivative infrared spectroscopy. *Anal. Biochem.* 340:89–98.
27. Noda, I. 1993. Generalized two-dimensional correlation method applications to infrared, Raman, and other types of spectroscopy. *Appl. Spectrosc.* 47:1329–1336.
28. Noda, I. 1989. Two-dimensional infrared spectroscopy. *J. Am. Chem. Soc.* 111:8116–8118.
29. Noda, I. 1990. Two-dimensional infrared (2D-IR) spectroscopy: theory and applications. *Appl. Spectrosc.* 44:550–561.
30. Czarnecki, M. A. 2000. Two-dimensional correlation spectroscopy: effect of band position, width, and intensity changes on correlation intensities. *Appl. Spectrosc.* 54:986–993.
31. He, H.-W., J. Zhang, H.-M. Zhou, and Y.-B. Yan. 2005. Conformational change in the C-terminal domain is responsible for the initiation of creatine kinase thermal aggregation. *Biophys. J.* 89:2650–2658.
32. Olinger, J. M., D. M. Hill, R. J. Jakobsen, and R. S. Brody. 1986. Fourier transform infrared studies of ribonuclease in H_2O and ^2H_2O solutions. *Biochim. Biophys. Acta.* 869:89–98.
33. Haris, P. I., D. C. Lee, and D. Chapman. 1986. A Fourier transform infrared investigation of the structural differences between ribonuclease A and ribonuclease S. *Biochim. Biophys. Acta.* 874:255–265.
34. Dong, A., R. M. Hyslop, and D. L. Pringle. 1996. Difference in conformational dynamics of ribonucleases A and S as observed by infrared spectroscopy and hydrogen-deuterium exchange. *Arch. Biochem. Biophys.* 333:275–281.
35. Reinstädler, D., H. Fabian, J. Backmann, and D. Naumann. 1996. Refolding of thermally and urea-denatured ribonuclease A monitored by time-resolved FTIR spectroscopy. *Biochemistry.* 35:15822–15830.
36. Schultz, C. P., H. Fabian, and H. H. Mantsch. 1998. Two-dimensional mid-IR and near-IR correlation spectra of ribonuclease A: Using overtones and combination modes to monitor changes in secondary structure. *Biospectroscopy.* 4:S19–S29.
37. Zhang, J., H.-W. He, Q. Wang, and Y.-B. Yan. 2006. Sequential events in ribonuclease A thermal unfolding characterized by two-dimensional infrared correlation spectroscopy. *Protein Peptide. Lett.* 14:33–40.
38. Wlodawer, A., L. A. Svensson, L. Sjölin, and G. L. Gilliland. Structure of phosphate-free ribonuclease A Refined at 1.26 Å. *Biochemistry.* 27:2705–2717.
39. Santoro, J., C. González, M. Bruix, J. L. Neira, J. L. Nieto, J. Herranz, and M. Rico. 1993. High-resolution three-dimensional structure of ribonuclease A in solution by nuclear magnetic resonance spectroscopy. *J. Mol. Biol.* 229:722–734.
40. Crestfield, A. M., W. H. Stein, and S. Moore. 1962. On the aggregation of bovine pancreatic ribonuclease. *Arch. Biochem. Biophys.* 1(Suppl.): 217–222.

41. Noda, I. 2004. Advances in two-dimensional correlation spectroscopy. *Vib. Spectroscopy.* 36:143–165.

42. Meersman, F., and K. Heremans. 2003. Temperature-induced dissociation of protein aggregates: accessing the denatured state. *Biochemistry.* 42:14234–14241.

43. Barth, A. 2000. The infrared absorption of amino acid side chains. *Prog. Biophys. Mol. Biol.* 74:141–173.

44. Torrent, J., P. Rubens, M. Ribó, K. Heremans, and M. Vilanova. 2001. Pressure versus temperature unfolding of ribonuclease A: An FTIR spectroscopic characterization of 10 variants at the carboxy-terminal site. *Protein Sci.* 10:725–734.

45. Stelea, S. D., P. Pancoska, A. S. Benight, and T. A. Keiderling. 2001. Thermal unfolding of ribonuclease A in phosphate at neutral pH: Deviations from the two-state model. *Protein Sci.* 10:970–978.

46. Cleland, J. F., and D. I. C. Wang. 1990. Refolding and aggregation of bovine carbonic anhydrase B: quasi-elastic light scattering analysis. *Biochemistry.* 29:11072–11078.

47. Chiti, F., N. Taddei, F. Baroni, C. Capanni, M. Stefani, G. Ramponi, and C. M. Dobson. 2002. Kinetic partitioning of protein folding and aggregation. *Nat. Struct. Biol.* 9:137–143.

48. Yan, Y.-B., Q. Wang, H.-W. He, and H.-M. Zhou. 2004. Protein thermal aggregation involves distinct regions: sequential events in the heat-induced unfolding and aggregation of Hemoglobin. *Biophys. J.* 86:1682–1690.

49. Uversky, V. N., and A. L. Fink. 2004. Conformational constraints for amyloid fibrillation: the importance of being unfolded. *Biochim. Biophys. Acta.* 1698:131–153.

50. Matheson, R. R., and H. A. Scheraga. 1979. Steps in the pathway of the thermal unfolding of ribonuclease A. A nonspecific photochemical surface-labeling study. *Biochemistry.* 18:2437–2445.

51. Navon, A., V. Ittah, J. H. Laity, H. A. Scheraga, E. Haas, and E. E. Gussakovsky. 2001. Local and long-range interactions in the thermal unfolding transition of bovine pancreatic ribonuclease A. *Biochemistry.* 40:93–104.

52. Burgess, A. W., L. I. Weinstein, D. Gabel, and H. A. Scheraga. 1975. Immobilized carboxypeptidase A as a probe for studying the thermally induced unfolding of bovine pancreatic ribonuclease. *Biochemistry.* 14:197–200.

53. Liu, Y., P. J. Hart, M. P. Schlunegger, and D. Eisenberg. 1998. The crystal structure of a 3D domain-swapped dimer of RNase A at a 2.1 Å resolution. *Proc. Natl. Acad. Sci. USA.* 95:3437–3442.